Eur Biophys J (2001) 30: 179–185
DOI 10.1007/s002490000121

ARTICLE

**Michaela Vorlíčková · Iva Kejnovská
Marcela Tumová · Jaroslav Kypr**

Conformational properties of DNA fragments containing GAC trinucleotide repeats associated with skeletal displasias

Received: 8 August 2000 / Revised version: 12 October 2000 / Accepted: 19 October 2000 / Published online: 15 December 2000

Abstract The human gene for cartilage oligomeric matrix protein contains five tandem repeats of the GAC trinucleotide. Its expansion by one repeat causes multiple epiphyseal dysplasia, while expansion by two repeats or, remarkably, deletion of one repeat causes pseudoachondroplasia. Here we used CD spectroscopy, PAGE and UV absorption spectroscopy to compare conformational properties of the DNA strands containing four, five, six and seven repeats of the GAC trinucleotide. The $(GAC)_n$ strands were found to form four distinct ordered conformations, depending on the solution conditions. The first was a foldback, stable at slightly alkaline pH values and low and medium ionic strengths. Increasing salt concentration induced a transition of the foldback into an antiparallel right-handed homoduplex. Both the conformers contained the Watson-Crick G·C pairs while the intervening adenines contributed little to their B-like conformation. Thirdly, the strands associated into a parallel homoduplex stabilized by the hemiprotonated C^+·C pairs and by the GpA steps that both favor the parallel DNA strand orientation. The parallel homoduplex was stable even at neutral pH. The fourth conformation was the left-handed Z-DNA, which formed easier with $(GAC)_n$ than with $(GC)_n$ of comparable length, indicating that the adenines of $(GAC)_n$ promoted the left-handed duplex. The paper shows that stability of the above four conformers strongly depends on the GAC repeat number.

Keywords DNA conformations · $(GAC)_n$ trinucleotide repeats · Circular dichroism · Epiphyseal displasia · Pseudoachondroplasia

M. Vorlíčková (✉) · I. Kejnovská · M. Tumová · J. Kypr
Institute of Biophysics of the Academy
of Sciences of the Czech Republic,
Královopolská 135, 61265 Brno, Czech Republic
E-mail: mifi@ibp.cz
Tel.: +420-5-41517188
Fax: +420-5-41240497

Introduction

Trinucleotide repeats have been an attractive object of many studies starting from the early 1990s, when it was shown that they expanded in genomes and that the expansions caused serious diseases. Attention was first focused on the $(CGG)_n$·$(CCG)_n$ repeats, whose expansions cause fragility of chromosome X (reviewed by, e.g. Sutherland et al. 1998). Then $(CAG)_n$·$(CTG)_n$ followed because their expansions cause Huntington chorea, myotonic dystrophy and several other, mostly neurodegenerative, diseases (reviewed by, e.g. Ashley and Warren 1995; Wells 1996; Kypr and Vorlíčková 1997; Timchenko and Caskey 1999). Thirdly, the family of disease-causing repeats was extended to $(GAA)_n$·$(TTC)_n$, whose expansions stand behind Friedreich ataxia (Campuzano et al. 1996; reviewed by, e.g. Kypr and Vorlíčková 1998). Simultaneously, computer studies of the genomic nucleotide sequences suggested that expansions were not restricted to the disease-causing trinucleotide repeats (Mrázek and Kypr 1994), and that the expansions even were not restricted to trinucleotide repeats at all because, for example, dinucleotide repeats expand much more in eukaryotic genomes than the trinucleotide repeats (Matula and Kypr 1999). It is now already known that microsatellite expansions are a sophisticated evolutionary device (Djian 1998) and that the diseases probably are the price that we pay for the existence of the expansion phenomenon that may have played an essential role in the evolution of the eukaryotic genomes (Matula and Kypr 1999).

Microsatellites can slip and adopt various other noncanonical conformations (e.g. Chastain et al. 1995; Mitas 1997; Gacy and McMurray 1998; Mariappan et al. 1998; Vorlíčková et al. 1998a, 1998b, 1999). The noncanonical DNA conformations are frequently thought to cause the expansions (Samadashwily et al. 1997; Pearson and Sinden 1998; McMurray 1999). In the above-mentioned diseases caused by the expansions of $(CCG)_n$·$(CGG)_n$, $(CAG)_n$·$(CTG)_n$ and $(GAA)_n$·$(TTC)_n$,

the disease alleles are very long, which makes it impossible to study their conformational properties by high-resolution methods. That is why it was interesting to encounter a report in the recent literature where pathological effects were caused by a very small repeat number change (Délot et al. 1999). Specifically, the human gene for cartilage oligomeric matrix protein contains five tandem repeats of the GAC trinucleotide. Its expansion by one repeat causes multiple epiphyseal dysplasia, while expansion by two repeats or, remarkably, deletion of one repeat causes pseudoachondroplasia (Délot et al. 1999). Here we examine conformational properties of the DNA strands containing the four, five, six and seven tandem repeats of the GAC trinucleotide.

Material and methods

The oligonucleotides were bought from the Laboratory of Plant Molecular Physiology, Faculty of Science, Masaryk University, Brno, Czech Republic. The lyophilized oligonucleotides were dissolved in 1 mM sodium phosphate + 0.3 mM EDTA, pH 7. Sample concentrations were determined from their absorption measured at 25 °C in the above buffer using the molar (per nucleoside residue) extinction coefficients (at 257 nm) of 9750, 9780, 9520 and 9400 M^{-1} cm^{-1} for $(GAC)_4$, $(GAC)_5$, $(GAC)_6$ and $(GAC)_7$, respectively. The molar extinction coefficients were determined from the molar extinction coefficients at 260 nm of single-stranded samples calculated according to Gray et al. (1995) that were multiplied by the ratio of the absorbance of the sample at the absorption maximum in the native and denatured state. The UV absorption spectra were measured on a Unicam 5625 UV/Vis spectrometer. CD spectra were measured using the Jobin-Yvon mark VI spectrometer in 0.1 cm pathlength Hellma cells placed in a thermostatted holder. Unless stated otherwise, all the measurements were done at 0 °C. Concentrations were around 0.8 mM in all samples. Ellipticity was expressed in M^{-1} cm^{-1}, the molarity being related to the nucleoside residues in the DNA samples.

Required volumes of concentrated sodium phosphate or Britton-Robinson buffer were added to the oligonucleotide samples to obtain the conditions given in the figure captions. The pH was adjusted by adding dilute HCl or NaOH to the cells, where it was directly measured using a Radelkis pH-meter and an Orion microelectrode. Salt concentrations were increased by adding concentrated salt solutions or known weights of solid salts directly into the cells. The salt and DNA concentrations were corrected for the sample volume increase.

Non-denaturing polyacrylamide gel electrophoresis was performed in a thermostatted apparatus (SE-600, Hoefer Scientific). Gels (20%, 29:1 monomer/bis ratio), 14 × 16 × 0.1 cm in size, were run for 20 h at 70 V (~5 V/cm) and 0 °C. DNA concentration was about 0.8 mM in the electrophoresed samples. The gels were stained with Stains-All from Sigma. Densitometry was performed using the Personal Densitometer SI, model 375-A (Molecular Dynamics).

Results

In mildly alkaline, low-salt solutions (pH~8, 1 mM sodium phosphate), $(GAC)_n$ ($n = 4$–7) provide B-like CD spectra (Fig. 1A). The spectra are conservative (the positive and negative bands approximately have the same magnitudes), having the positive and negative maxima at 280 nm and 258 nm, respectively. The spectra differ from those calculated for denatured $(GAC)_n$ strands (Fig. 1A) and they are strongly dependent on temperature (Fig. 1A). The temperature changes are reversible and the thermal stability of the $(GAC)_n$ samples increases with their strand length (not shown). Electrophoretic results (Fig. 2A) demonstrate that all

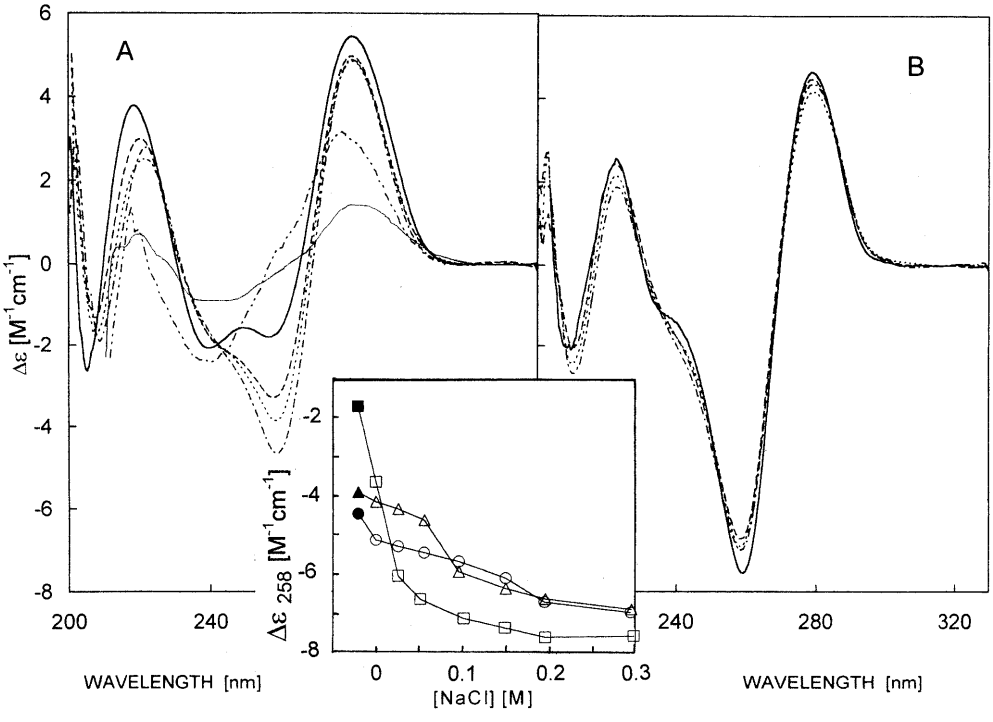

Fig. 1 CD spectra of $(GAC)_n$ measured at slightly alkaline pH values and **A** low and **B** high ionic strengths: *full trace* $(GAC)_4$, *dots* $(GAC)_6$, *dashes* $(GAC)_5$ and *dash-dot* $(GAC)_7$ in: **A** 1 mM sodium phosphate and 0.3 mM EDTA, pH 8.0 with $(GAC)_4$, and pH 7.5 with the other $(GAC)_n$; *dash, dot, dot* spectrum calculated for the $(GAC)_7$ single strand according to Cantor et al. (1970); *thin line* $(GAC)_7$ measured at 85 °C; **B** 10 mM sodium phosphate, 0.3 mM EDTA and 0.3 M NaCl, pH 8.0 with $(GAC)_4$, and pH 7.5 with the other $(GAC)_n$. *Insert*: salt-induced changes of the negative CD band depth: *squares* $(GAC)_4$, *triangles* $(GAC)_6$ and *circles* $(GAC)_7$. *Full* and *open symbols* correspond to samples containing 1 mM and 10 mM sodium phosphate, respectively. All the spectra and points in the dependences correspond to equilibrium

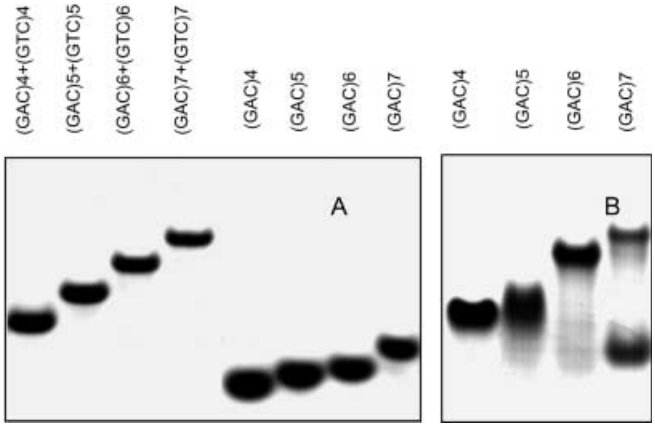

Fig. 2 Native electrophoresis of $(GAC)_n$ run at slightly alkaline pH values: **A** 1 mM sodium phosphate and 0.3 mM EDTA, pH 8; **B** Britton-Robinson buffer and 0.34 M NaCl, pH 8. Heteroduplexes of $(GAC)_n$ with the complementary $(GTC)_n$ strands serve as the length markers

the $(GAC)_n$ samples are single stranded under these experimental conditions. We conclude that they are foldbacks.

If the ionic strength is increased in the slightly alkaline solutions, then PAGE demonstrates the formation of bimolecular duplexes with all four $(GAC)_n$ fragments present (Fig. 2B). The salt-induced changes are accompanied by a decrease of the positive band and, especially, by a deepening of the negative CD band at 258 nm (compare Fig. 1A and B). The dodecamer $(GAC)_4$ transforms into the duplex at a lower salt concentration than the longer $(GAC)_n$ fragments (Fig. 1, insert). The transition is faster than one can detect by conventional CD (its foldback is not very stable). The transitions of the longer fragments are slow. $(GAC)_5$ and $(GAC)_6$ transform at similar salt concentrations [the dependence for $(GAC)_6$ is only shown in the insert of Fig. 1] and the equilibrium is attained within 1 and 4–5 h, respectively. The transition of $(GAC)_7$ lasts about a day. The low-salt CD spectra of the $(GAC)_n$ oligonucleotides become similar to the CD spectra of the duplexes with the increasing oligonucleotide length because the foldback stem gets longer and the contribution of the foldback loop is smaller. Electrophoretic results (Fig. 2B) are in line with the CD results. Dodecamer $(GAC)_4$ is completely a duplex under the conditions when about a half of the $(GAC)_7$ molecules still persist in the foldback. The foldback-duplex transition takes a longer time with the increasing oligonucleotide length to provide two separate electrophoretic bands corresponding to the foldback and the bimolecular duplex.

At moderate concentrations of salt, the CD spectra of $(GAC)_n$ become remarkably similar to the CD spectra of $(GC)_n$ (Figs. 1B and 3). Hence $(GAC)_n$ associate into antiparallel duplexes containing the Watson G·C pairs, whereas the intervening adenines contribute little to the duplex conformation. Yet the same electrophoretic mobility of the $(GAC)_n$ homoduplexes and of their heteroduplexes with the complementary $(GTC)_n$ strands (Fig. 2A, B) indicates that the opposite adenines probably remain intrahelical because extrahelical bases modify the electrophoretic mobility (our unpublished data).

Molar salt concentrations caused dramatic changes in the CD spectra of $(GAC)_n$ (Figs. 3 and 4). The negative 258 nm band disappeared and a negative band appeared in the long wavelength region. This process was complete with all the $(GAC)_n$ at about 4 M NaCl. The transition midpoint was slightly shifted to lower salt concentrations with the increasing fragment length (Fig. 4). Simultaneously, the kinetics was influenced by the fragment length, being fast with $(GAC)_4$ (faster than it could be detected by the conventional CD spectrometer) and slow (hours) with $(GAC)_7$. Experiments with $(GC)_5$ (Fig. 3A) and $(GC)_{10}$ (Fig. 3D) demonstrated that $(GAC)_n$ isomerized to the left-handed Z-DNA. It is remarkable that the $(GAC)_n$

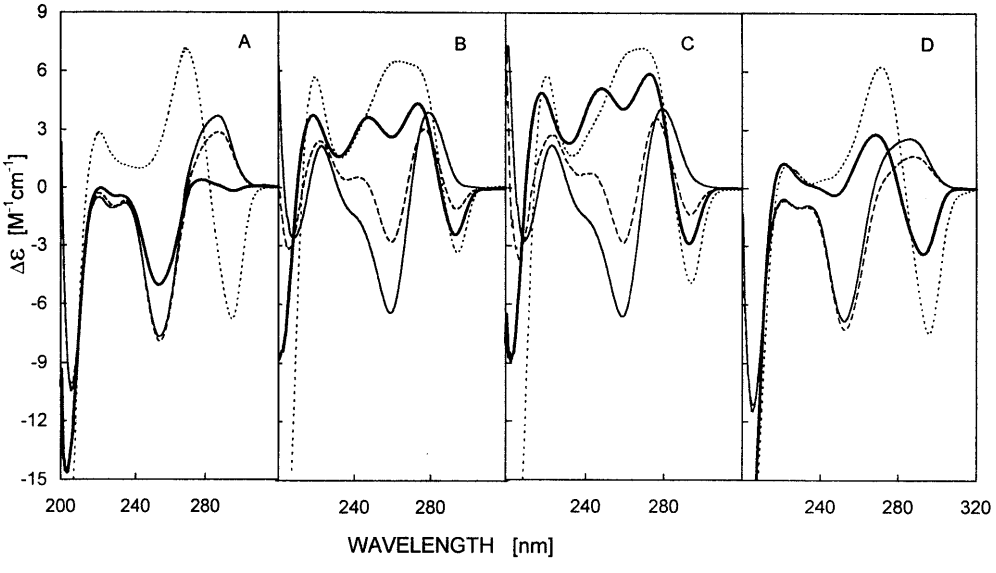

Fig. 3 CD spectra of $(GC)_n$ and $(GAC)_n$ in the course of their transition to the Z-form: **A** $(GC)_5$ in 10 mM sodium phosphate, 0.3 mM EDTA, pH 7 and *full trace* 0, *dashes* 0.76, *thick full trace* 5 M NaCl and *dots* 5 M NaCl + 0.2 mM $NiCl_2$; **B** $(GAC)_4$, **C** $(GAC)_7$ and **D** $(GC)_{10}$ in *full trace* 0.3, *dashes* 2, *thick full trace* 4 M NaCl and *dots* 4 M NaCl + 0.4 mM $NiCl_2$. All of the spectra were recorded at equilibrium

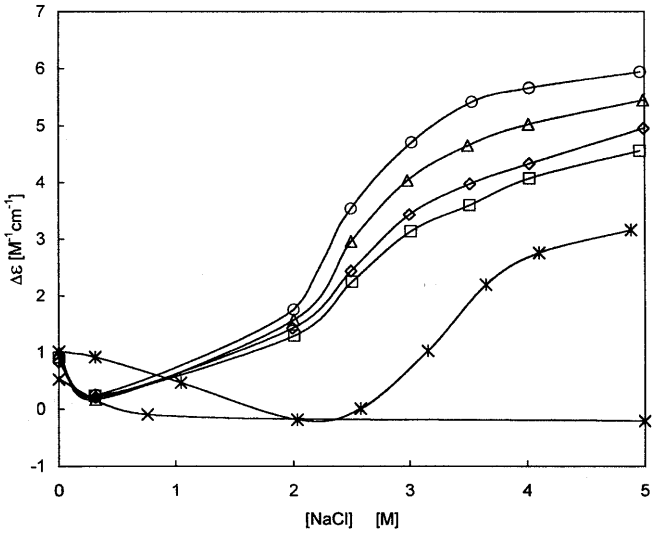

Fig. 4 Ellipticity changes at 270 nm during the NaCl-induced transition of $(GAC)_n$ and $(GC)_n$ to the Z-form: *squares* $(GAC)_4$, *rhombs* $(GAC)_5$, *triangles* $(GAC)_6$, *circles* $(GAC)_7$, *asterisks* $(GC)_{10}$ and *crosses* $(GC)_5$. Experimental conditions are the same as in Fig. 3. The points are all at equilibrium that was reached immediately with $(GAC)_4$ and $(GAC)_5$, within 24 h with $(GAC)_6$ and within 48 h with $(GAC)_7$ and $(GC)_{10}$. No transition was observed in NaCl with $(GC)_5$

homoduplexes were switched into Z-DNA even by NaCl, i.e. in the absence of $NiCl_2$, whereas $(GC)_{10}$ was the first member of the $(GC)_n$ family that did not need $NiCl_2$ to switch into Z-DNA (Fig. 3D). Neither $(GC)_4$ (not shown) nor $(GC)_5$ (Figs. 3A and 4) isomerized into the Z-form in mere NaCl. Only $NiCl_2$ triggered this transition (Fig. 3A), which had long kinetics (the equilibrium was only reached after 24 h). Addition of $NiCl_2$ also caused changes in the CD spectra of $(GAC)_n$. In contrast to NaCl, the $NiCl_2$-induced changes were as slow as with $(GC)_n$ with all the four lengths of the present $(GAC)_n$ fragments. The resulting CD spectra had much larger amplitudes in NaCl + $NiCl_2$ than in NaCl. We think that NaCl induced a variant of Z-DNA other than NaCl + $NiCl_2$ did. The experiments demonstrated that the mispaired adenines of $(GAC)_n$ catalyzed the DNA isomerization into the left-handed Z-form. $(GAC)_n$ also were switched into the Z-form by $MgCl_2$ (not shown). This transition was remarkably fast (kinetics not measurable by CD) with all the four present oligonucleotides. Its cooperativity slightly increased with the fragment length, being very low (nearly linear dependence) with $(GAC)_4$, while the half-width of the transition was about 0.2 M Mg^{2+} with $(GAC)_7$. Interestingly, the transition midpoints were the same, about 0.6 M $MgCl_2$, with the shortest and the longest oligonucleotide, while they were about 0.8 and 0.85 M $MgCl_2$ with $(GAC)_5$ and $(GAC)_6$, respectively.

Another kind of dramatic CD change was observed if the $(GAC)_n$ were transferred from the slightly alkaline to neutral, or slightly acid, pH solutions (Fig. 5). Even in 1 mM Na phosphate, pH 7, the CD spectrum of $(GAC)_4$ provided large, blue-shifted bands compared to the longer $(GAC)_n$ fragments (see below). Exposure of $(GAC)_4$ to more alkaline pH eliminated this difference (Fig. 1A). The behavior of $(GAC)_4$ suggested that the repeats were prone to protonation even at neutral pH. Hence we studied the effects of protonation on the behavior of $(GAC)_n$.

CD spectra recorded with $(GAC)_4$ at various pH values from 8.2 to 5.0 (Fig. 5A) showed that the dodecamer underwent extensive pH-induced changes. At the end of this transition, i.e. at a pH of about 5.5, the dodecamer provided a huge conservative CD spectrum with an ellipticity of about 18 M^{-1} cm^{-1} around 260 nm,

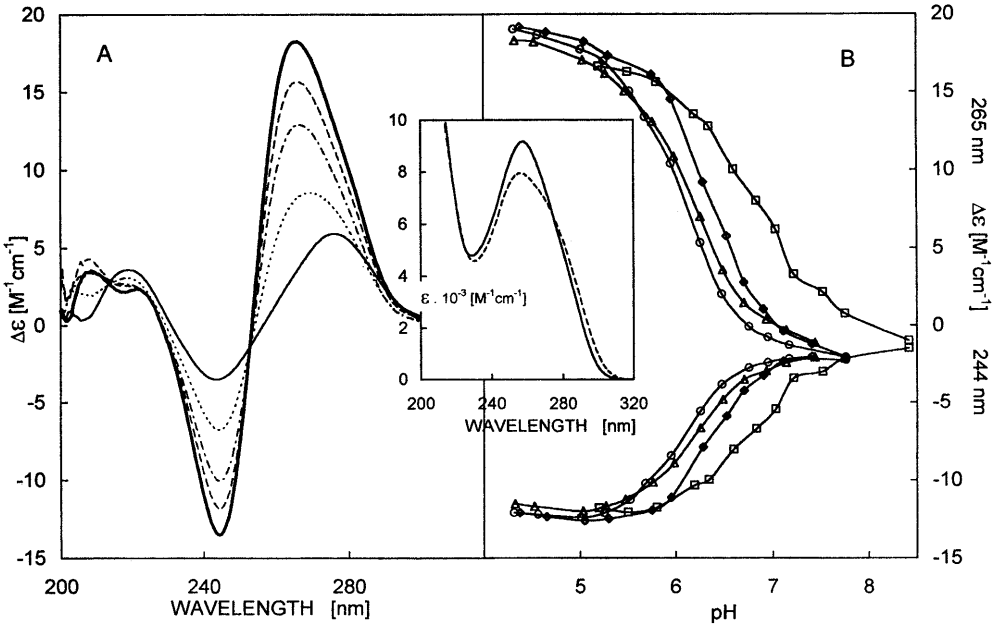

Fig. 5A, B Transitions of $(GAC)_n$ to the parallel-stranded homoduplex: the pH-induced transitions were recorded in 1 mM Na phosphate and 0.3 mM EDTA. **A** CD spectra in the course of the transition of $(GAC)_4$: pH *full trace* 7.2, *dots* 6.8, *dash-dot* 6.3, *dashes* 5.8 and *thick full trace* 5.0. *Insert*: UV absorption spectra of $(GAC)_4$ at pH *full trace* 7.2 and *dashes* 5.8. **B** The pH-induced transitions of *squares* $(GAC)_4$, *rhombs* $(GAC)_5$, *triangles* $(GAC)_6$ and *circles* $(GAC)_7$

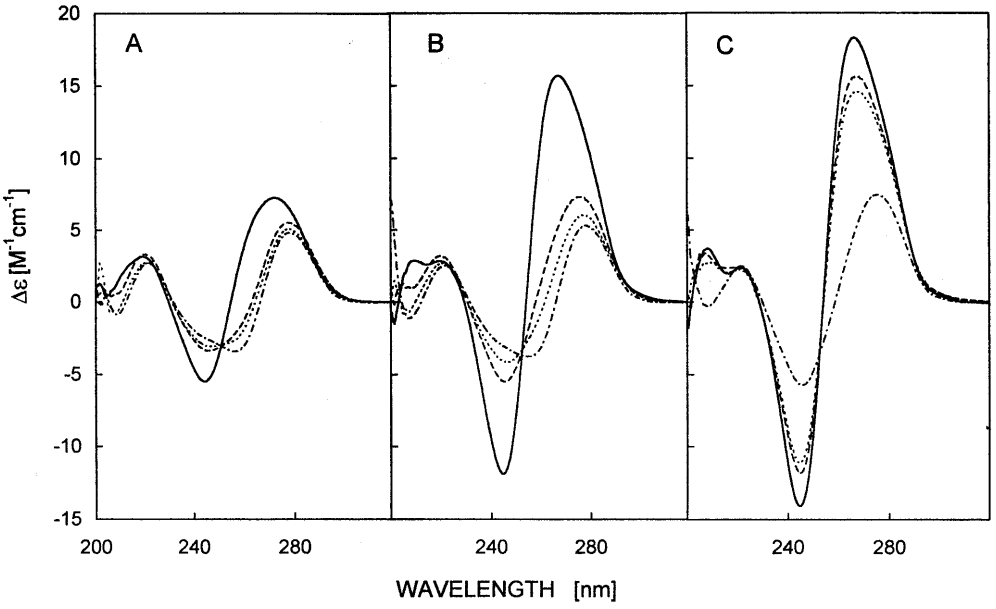

Fig. 6 CD spectra of $(GAC)_n$ recorded at neutral pH values: *full trace* $(GAC)_4$, *dashes* $(GAC)_5$, *dots* $(GAC)_6$ and *dash-dot* $(GAC)_7$ in: **A** 1 mM sodium phosphate and 0.3 mM EDTA, pH 6.9; **B** 10 mM sodium phosphate and 0.3 mM EDTA, pH 6.9. The spectra were measured immediately after increasing the buffer concentration. **C** Equilibrium spectra of the samples presented in **B** which were taken 24 h after increasing the buffer concentration

which was an almost 10 times larger amplitude than we obtained with, for example, native calf thymus DNA and much larger than with any antiparallel duplex DNA. Essentially the same CD spectrum was observed with CGACGAC around pH 5, where NMR spectroscopy showed that the heptamer associated into a parallel-stranded homoduplex (Robinson and Wang 1993). The acid-induced changes were hypochromic (Fig. 5, insert), indicating that the bases properly stacked in the parallel-stranded homoduplex. The shoulder at 285 nm in the UV absorption spectrum suggested that parallel duplex formation by $(GAC)_4$ was accompanied by cytosine protonation. Figure 5B compares the acid-induced transition of the four present $(GAC)_n$ fragments to demonstrate that the midpoint was shifted to more acid values with the increasing DNA strand length.

Unlike the longer $(GAC)_n$ repeats, $(GAC)_4$ provided a non-negligible amount of the parallel-stranded homoduplex even at pH 7 (Figs. 5B and 6A). It follows from electrophoretic experiments (Fig. 7A) that the stable foldbacks of longer $(GAC)_n$ fragments hindered their switch into the parallel protonated homoduplex. Increasing the ionic strength to 10 mM sodium phosphate (Fig. 6B) shifted the pH-induced transition to more neutral pH values and made the differences between the four $(GAC)_n$ strands still larger. In addition, the spectra changed with time. $(GAC)_4$ reached equilibrium (Fig. 6C) after 1 h whereas it took 40 h to obtain equilibrium with the other three $(GAC)_n$ repeats. The equilibrium CD spectrum (at pH 6.9) was the largest with $(GAC)_4$ followed by $(GAC)_5$ and $(GAC)_6$, while the amplitudes of $(GAC)_7$ were still rather small (Fig. 6C). The three shorter $(GAC)_n$ fragments were completely associated into the parallel homoduplex even at pH 6.5 in 0.15 M KCl and 6 mM $MgCl_2$, i.e. under almost physiological conditions. Electrophoretic results obtained in acid gels (Fig. 7) were entirely consistent

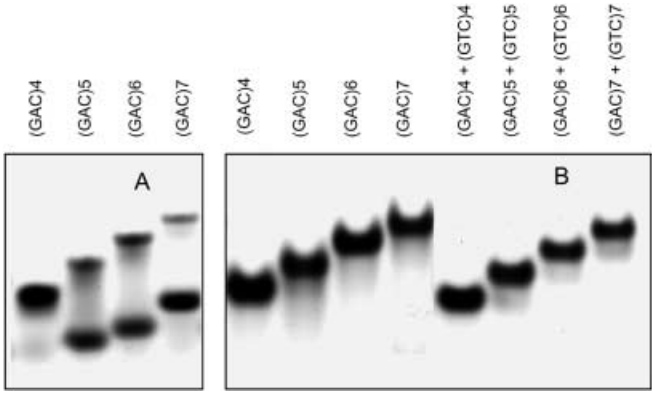

Fig. 7 Native electrophoresis of $(GAC)_n$ in slightly acidic gels: **A** 1 mM sodium phosphate and 0.3 mM EDTA, pH 6.7; **B** Britton-Robinson buffer and 0.3 M NaCl, pH 6.3. Duplexes of $(GAC)_n$ with the complementary $(GTC)_n$ strands served as the length markers

with the conclusions following from the CD experiments. At pH 6.7, $(GAC)_4$ was almost completely a duplex at low salt while longer $(GAC)_n$ fragments provided bands corresponding to both foldback and duplex. The amount of foldback increased with the fragment length. If the pH value was lower and the ionic strength higher, then all four fragments associated into the duplex. The parallel homoduplexes of $(GAC)_n$ migrated slightly slower than the antiparallel heteroduplexes of $(GAC)_n$ with $(GTC)_n$. The slower migration was also observed with the parallel homoduplex of $(GA)_n$ (Ortiz-Lombardia et al. 1995).

Discussion

This work presents results of a comparative study of the conformations that the $(GAC)_n$ ($n = 4$–7) DNA strands

can adopt under various conditions in solution. The conformational space of the fragments is found to contain four basic conformers. The first two, i.e. the foldback and the antiparallel duplex, are both based on Watson pairing of G with C. The adenines contribute little to the properties of these two conformers, though they are probably not bulged out from the duplex. As usual, the foldback-duplex equilibria are influenced by the ionic strength (Fig. 2A, B), the DNA fragment length (Fig. 2B) and DNA concentration (not shown).

The third conformer is the parallel homoduplex containing hemiprotonated cytosine homopairs. The parallel homoduplex is also stabilized by the GA steps because the $(CAG)_n$ fragments (i.e., containing the AG steps) do not associate into the parallel homoduplex and instead form a very stable foldback even at acid pH values (Vorlícková et al. 1998b). The parallel homoduplex of $(GAC)_n$ is even stable at neutral pH values (Fig. 6). The isomerization of $(GAC)_n$ from the parallel to the antiparallel duplex, or back, is a complex process lasting hours, the time being dependent on the fragment length. The parallel homoduplex of $(GAC)_n$ is the same as that of the heptamer CGACGAC at pH 5 that was characterized by NMR (Robinson and Wang 1993).

The fourth (and last) conformer adopted by $(GAC)_n$ in solution is rather surprisingly the left-handed Z-DNA. Even more interesting is the present observation that the unpaired adenine catalyzes the transition to Z-DNA, which to the best of our knowledge is the first example of a molecule whose Z-DNA is promoted by an unpaired base. Of course, the present observation inspired experiments with "mutants" of $(GAC)_n$ in which other bases than A, or even longer unpaired runs of A, were tested for their catalytic effect on the formation of Z-DNA. The results of these studies will be reported elsewhere.

The present studies were inspired by our previous studies of the DNA strands containing the $(GA)_n$, $(CGA)_n$ or $(CAG)_n$ repeats (Vorlícková et al. 1998a, 1998b, 1999) and by a recent demonstration that the human gene for cartilage oligomeric matrix protein contains five tandem repeats of the GAC trinucleotide (Délot et al. 1999). Its expansion by one repeat causes multiple epiphyseal dysplasia while expansion by two repeats or, remarkably, deletion of one repeat causes pseudoachondroplasia. The above results demonstrate that the conformational space of all four present fragments is composed of four conformers, but that the conformational equilibria are strongly dependent on the $(GAC)_n$ repeat number. It is difficult even to speculate whether the repeat number-dependent conformational preferences have something in common with the pathological properties. There are two rather more straightforward possibilities. The first is the aspartic acid run encoded by $(GAC)_n$ in the cartilage oligomeric matrix protein, whose change in length can of course cause the pathological effects. The second possibility is the fact that addition or deletion of one or two trinucleotide repeats dramatically influences the relative orientation of the double helix faces preceding and following the repeat. This can abolish or even establish dimerization of proteins, one of which binds to DNA in front of the repeat and the other behind the repeat.

Another problem is how the $(GAC)_5$ repeat allele of the healthy individuals is changed into the pathological $(GAC)_4$, $(GAC)_6$ and $(GAC)_7$ variants. In this process the conformational polymorphism of the $(GAC)_n$ repeats described above could have a role. However, the $(GAC)_5$ expansion and shortening occurs in vivo in the presence of the complementary $(GTC)_5$ strand. Its studies and studies of the $(GAC)_n \cdot (GTC)_n$ duplexes are in progress.

Acknowledgements This work was supported by grant 204/98/1027 provided by the Grant Agency of the Czech Republic.

References

Ashley CT Jr, Warren ST (1995) Trinucleotide repeat expansion and human disease. Annu Rev Genet 29: 703–728

Campuzano V, Montermini L, Moltó MD, Pianese L, Cossée M, Cavalcanti F, Monros E, Rodius F, Duclos F, Monticelli A, Zara F, Canñizares J, Koutnikova H, Bidichandani SI, Gellera C, Brice A, Trouillas P, DeMichele G, Filla A, DeFrutos R, Palau F, Patel PI, DiDonato S, Mandel J-L, Cocozza S, Koenig M, Pandolfo M (1996) Friedreich's ataxia: autosomal recessive disease caused by an intronic GAA triplet repeat expansion. Science 271: 1423–1427

Cantor CR, Warshaw MM, Shapiro H (1970) Oligonucleotide interactions. 3. Circular dichroism studies of the conformation of the deoxyoligonucleotides. Biopolymers 9: 1059–1077

Chastain PD II, Eichler EE, Kang S, Nelson DL, Levene SD, Sinden RR (1995) Anomalous rapid electrophoretic mobility of DNA containing triplet repeats associated with human disease genes. Biochemistry 34: 16125–16131

Délot E, King LM, Briggs MD, Wilcox WR, Cohn DH (1999) Trinucleotide expansion mutations in the cartilage oligomeric matrix protein (COMP) gene. Hum Mol Genet 8: 123–128

Djian P (1998) Evolution of simple repeats in DNA and their relation to human disease. Cell 94: 155–160

Gacy AM, McMurray CT (1998) Influence of hairpins on template reannealing at trinucleotide repeat duplexes: a model for slipped DNA. Biochemistry 37: 9426–9434

Gray DM, Hung SH, Johnson KH (1995) Absorption and circular dichroism spectroscopy of nucleic acid duplexes and triplexes. Methods Enzymol 246: 19–34

Kypr J, Vorlícková M (1997) Conformational properties and expansion of DNA molecules containing tandem repeats of triplets starting by cytosine and ending with guanine. Chem Listy 91: 570-574

Kypr J, Vorlícková M (1998) Conformational properties of DNA strands containing guanine and adenine. Chem Listy 92: 530–537

Mariappan SVS, Silks LA III, Chen X, Springer PA, Wu R, Moyzis RK, Bradbury EM, Garcia AE, Gupta G (1998) Solution structures of the Huntington's disease DNA triplets, $(CAG)_n$. J Biomol Struct Dyn 15: 723–744

Matula M, Kypr J (1999) Nucleotide sequences flanking dinucleotide microsatellites in the human, mouse and drosophila genomes. J Biomol Struct Dyn 17: 275–280

McMurray CT (1999) DNA secondary structure: a common and causative factor for expansion in human disease. Proc Natl Acad Sci USA 96: 1823–1825

Mitas M (1997) Trinucleotide repeats associated with human disease. Nucleic Acids Res 25: 2245–2253

Mrázek J, Kypr J (1994) Length expansion is a general property of simple sequence repeats in eukaryotic genomes. Miami BioTechnol Short Rep 5: 39–39

Ortiz-Lombardia M, Eritja R, Azorín F, Kypr J, Tejralová I, Vorlícková M (1995) Divalent zinc cations induce the formation of two distinct homoduplexes of a $d(GA)_{20}$ DNA sequence. Biochemistry 34: 14408–14415

Pearson CE, Sinden RR (1998) Trinucleotide repeat DNA structures: dynamic mutations from dynamic DNA. Curr Opin Struct Biol 8: 321–330

Robinson H, Wang AH-J (1993) 5′-CGA sequence is a strong motif for homo base-paired parallel-stranded DNA duplex as revealed by NMR analysis. Biochemistry 90: 5224–5228

Samadashwily GM, Raca G, Mirkin SM (1997) Trinucleotide repeats affect DNA replication in vivo. Nat Genet 17: 298–304

Sutherland GR, Baker E, Richards RI (1998) Fragile sites still breaking. Trends Genet 14: 501–506

Timchenko LT, Caskey CT (1999) Triplet repeat disorders: discussion of molecular mechanisms. Cell Mol Life Sci 55: 1432–1447

Vorlícková M, Kejnovská I, Kovanda J, Kypr J (1998a) Conformational properties of DNA strands containing guanine-adenine and thymine-adenine repeats. Nucleic Acids Res 26: 1509–1514

Vorlícková M, Zimulová M, Kovanda J, Fojtík P, Kypr J (1998b) Conformational properties of DNA dodecamers containing four tandem repeats of the CNG triplets. Nucleic Acids Res 26: 2679–2685

Vorlícková M, Kejnovská I, Kovanda J, Kypr J (1999) Dimerization of the guanine-adenine repeat strands of DNA. Nucleic Acids Res 27: 581–586

Wells RD (1996) Molecular basis of genetic instability of triplet repeats. J Biol Chem 271: 2875–2878